Analysis of a Relay Operation for an Intercircuit Fault

Ryan McDaniel
Schweitzer Engineering Laboratories, Inc.

Analysis of a Relay Operation for an Intercircuit Fault

Ryan McDaniel, *Schweitzer Engineering Laboratories, Inc.*

Abstract—**During a winter snowstorm, a large amount of snow fell across a fairly small region in the Midwest of the United States. The temperatures and wind conditions were such that the snow accumulated vertically on transmission lines in the affected area, leading to large line sags in the transmission and subtransmission systems. Shortly after the snow accumulation ended, the temperatures warmed rapidly, causing the snow to melt. As large sections of snow fell off the underbuild subtransmission line, the subtransmission line came in contact with the transmission line above, creating an intercircuit fault.**

An intercircuit fault is a rare fault type in which phases from two circuits sharing the same right of way come in contact with each other. In this paper, we use gathered event reports to analyze an intercircuit fault that occurred multiple times between two separate voltage levels after the snowstorm. We also provide a detailed analysis of the mho element behavior for this fault and investigate the performance of different mho element polarizing techniques. The performance of the directional element and impedance-based fault location is examined. Furthermore, symmetrical components are used to verify the fault current and voltages for this intercircuit fault. Improvements to relay performance during intercircuit faults, including line current differential, are discussed.

I. INTRODUCTION

A late winter snowstorm in the Midwest led to hundreds of relay operations in a relatively small geographical area. The snowstorm was unusual in that there was wet, heavy snow (air temperature was slightly above freezing) and very little wind, which led to ideal conditions for very fast accumulation. Total snow accumulations varied widely, but some areas saw over 15 inches of snow in less than 48 hours. The snow managed to accumulate on power lines, which led to sags on the lines, and the lines came in contact with various surfaces to create faults. Nearly all relay operations that day were correct in that the relay cleared the faulted line. However, this paper discusses one of the relay misoperations that occurred. Once the root cause of the misoperation is identified by analyzing the event reports, a discussion of how to address unusual fault types is presented.

The utility that originally presented the author with the relay misoperation data has asked to not be mentioned. However, the utility has graciously allowed the author to use their data in anonymity to share the lessons we learned from this event.

II. SYSTEM OVERVIEW

Fig. 1 shows the 161 kV system with the fault marked on Line BC.

Line AB = 6.79 miles
Z1L = 0.0197∠80.63
Z0L = 0.056∠72.98

Line BC = 5.92 miles
Z1L = 0.0170∠80.2
Z0L = 0.0461∠72.2

All Impedances in Per Unit, 100 MVA Base
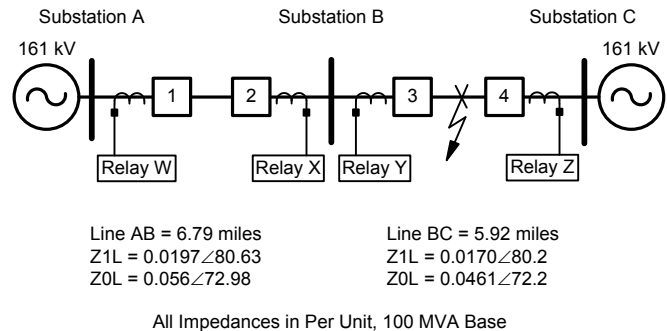
Fig. 1. Simplified one-line diagram of 161 kV system

Relays Y and Z are line current differential relays protecting Line BC. Relays W and X are distance relays with a permissive overreaching transfer trip (POTT) scheme protecting Line AB. In a POTT scheme, each relay must see the fault within its Zone 2 element for the line to trip at high speed. Upon Zone 2 pickup, the relay sends permission to the remote terminal. If a relay receives permission while its Zone 2 element is picked up, the relay is allowed to trip.

III. ANALYSIS

During a 75-minute window of time, eight faults occurred on Line BC and were cleared correctly by line current differential. For two of these faults, Relay W overreached and isolated Line AB. Fig. 2 shows the event history from the line current differential Relay Z.

We can see that the operations occur in pairs in which there is an initial operation, a reclose, and then a second operation. In the two cases where Relay W overreaches Line AB, Line BC had just reclosed. Line BC is reclosed at high speed from Breaker 3 and then followed 30 seconds later by Breaker 4. The overreaching misoperation occurs when Line BC is single-ended from the left source.

```
#    TIME        EVENT  LOCAT    CURR    FREQ   GRP  SHOT  TARGETS   Comment
1 13:11:04.020   AG T  $$$$$$      1   59.96    1    0      87      Remote Misop
2 13:11:00.048   AG T   3.48    4838   60.00    1    0      87

3 12:12:37.588   CG T  $$$$$$      1   60.01    1    0      87
4 12:12:33.375   CG T   3.44    4832   60.02    1    0      87

5 12:07:42.430   AG T  $$$$$$      1   59.99    1    0      87      Remote Misop
6 12:07:41.522   AG T   3.70    4804   59.99    1    0      87

7 11:45:27.693   AG T  $$$$$$      1   59.96    1    0      87
8 11:45:26.942   AG T   2.99    5100   59.99    1    0      87
```

Fig. 2.   Event history from Relay Z

A. Relay W Analysis for the Most Recent Fault

Going forward, we focus on Event #1, the most recent event to occur on the system. We will first start by analyzing Relay W.

1) Relay W Event Report History

Fig. 3 shows the event report history for Relay W, with the two events that resulted in a relay overreach noted. We can see that the times reported by Relay W do not correlate with the absolute relay times at Relay Z, but the relative time between events is identical. We note that Relay Z is 1:00:53.656 faster than Relay W. Relay Z is not connected to an IRIG-B source, but Relay W is.

```
#    TIME        EVENT  LOCAT  CURR   Comment
1 12:10:10.354   AG T   2.76   3854   Overreach
2 12:10:06.397   AG     5.98   2832

3 11:11:43.929   CG     4.60   3434
4 11:11:39.734   CG     6.28   2736

5 11:06:48.773   AG T   2.66   3890   Overreach
6 11:06:47.881   AG     5.84   2866

7 10:44:34.018   AG     5.34   3256
8 10:44:33.305   AG     6.70   2690
```

Fig. 3.   Event history from Relay W

The utility calculated the maximum phase-to-ground fault current contribution from Substation A with a fault at Substation B and Substation C open as 3,225 A. We can see that all reclose events exceed this value, with Events #1 and #5 having the largest excess. The fault current seen by the relay exceeds the expected fault current by as much as 20 percent.

The fault location reported by the relay for the two overreaching events is significantly lower than the line length of 6.49 miles, with Event #5 having a fault location of 40 percent from Substation A on Line AB. The impedance-based fault location method is extremely accurate when the fault is supplied from a single terminal. So the question is, why are we seeing greater than expected fault currents and fault location errors?

2) Relay W Event #1 Analysis

Fig. 4 shows the filtered event report for Event #1 at Relay W. A quick visual inspection shows A-phase current is elevated and A-phase voltage is depressed—the basic characteristics we expect for an A-phase-to-ground fault.
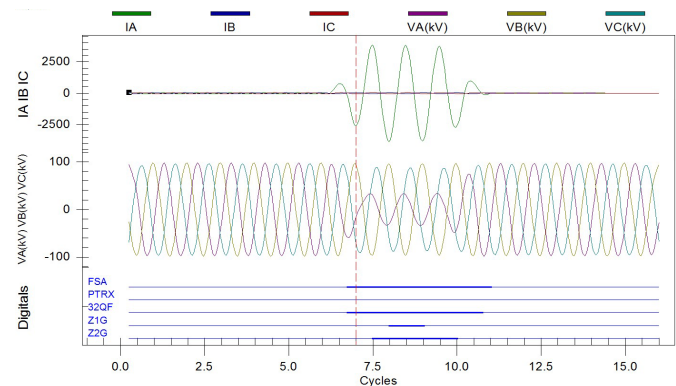
Fig. 4.   Event #1 from Relay W

Some of the key settings that will be used going forward are shown below. These include the line impedance parameters (Z1MAG, Z1ANG, Z0MAG, and Z0ANG) entered into the relay, the reach of the Zone 1 ground element (Z1G), and the directional element setting. The impedance settings are in ohms secondary.

CTR = 240
PTR = 800.00
Z1MAG = 1.53
Z1ANG = 80.63
Z0MAG = 4.35
Z0ANG = 73.93
LL = 6.79
E32 = AUTO
Z1G = 1.30

a) Fault Selection Logic

The relay fault identification logic declares an A-phase-to-ground fault with the assertion of the relay element FSA. A detailed discussion of the fault selection logic, which uses the angle measurement between the negative-sequence current (I_2) and zero-sequence current (I_0) to determine the faulted phase, is given in [1]. When A-phase is used as the reference phase for the sequence calculation and I_2 and I_0 are in phase, the relay declares an A-phase fault. In this example, $\angle I_2$ equals $\angle I_0$, which declares an A-phase fault.

b) Negative-Sequence Impedance Directional Element

The relay negative-sequence directional element declares this fault as a forward fault (32QF). A detailed discussion of this element is given in [2]. The negative-sequence impedance (Z_2) used by the directional element is calculated using (1).

$$Z_2 = \frac{\mathrm{Re}\left[V_2 \bullet (I_2 \bullet 1\angle\Theta)*\right]}{\left|I_2\right|^2} \qquad (1)$$

The relay element 32QF asserts when the calculated Z_2 value is less than the setting threshold Z2F. With the directional element set to automatic, E32 equals AUTO and the Z2F threshold is set at half of Z1MAG. Therefore, Z2F = 0.77 ohms secondary.

We can use a mathematical program to plot the Z_2 calculated by the relay for this fault using (1). The result of plotting Z_2 for this fault is shown in Fig. 5. The calculated Z_2 is –6.6 ohms, which is lower than Z2F.
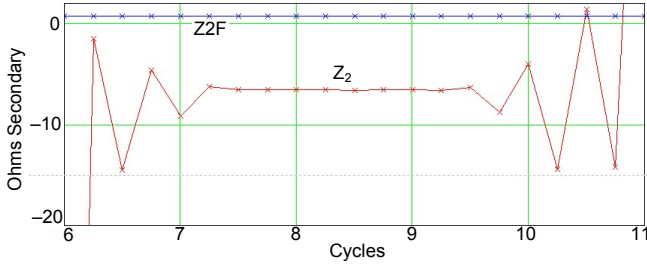
Fig. 5. Z_2 evaluation for Event #1 from Relay W

c) Ground Mho Element

Relay W uses a positive-sequence memory-polarized mho distance element to provide ground fault protection. There are many advantages to using this type of polarizing technique, with the major advantage being mho circle expansion, which leads to very good resistance relay coverage in weak systems. A more detailed discussion of memory-polarized relays can be found in [3].

The ground distance element can be modeled with (2) [4].

$$ZG = m \bullet \left|Z1L\right| = \frac{\mathrm{Re}\left[V_\phi \bullet (V_{1mem})*\right]}{\mathrm{Re}\left[1\angle Z1L \bullet (I_\phi + k_0 \bullet I_r) \bullet (V_{1mem})*\right]} \qquad (2)$$

The result of this equation is then plotted against the Zone 1 reach threshold, Z1G, in Fig. 6 [4].
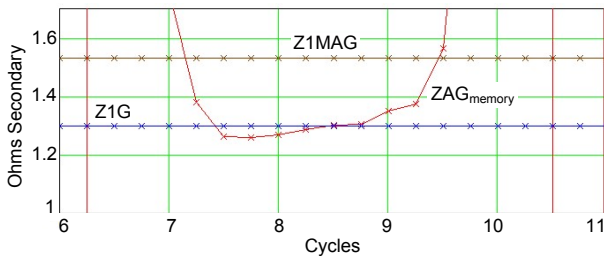
Fig. 6.   Ground distance reach evaluation for Event #1 from Relay W

We can see that the plotted reach is lower than the set point of Z1G for a short amount of time. This is similar to the

operations of the Z1G word bit viewed from the event report in Fig. 4.

d) Impedance and Resistivity Calculations

In addition to the operation of the relay protection elements, it is also valuable to calculate the apparent resistance and impedance of the fault. The impedance calculation is directly used in the fault location algorithm to calculate the distance to the fault. High resistance can adversely affect the fault location algorithm. Many techniques are used to mitigate the effects of resistance in single-ended fault locating methods [5]. This particular relay uses a modified Takagi method to calculate line impedance, and the formula to calculate impedance based on this method is shown in (3).

$$XG = m \bullet \left|Z1L\right| = \frac{\mathrm{Im}\left[V_\phi \bullet (I_r \bullet e^{j \bullet T})*\right]}{\mathrm{Im}\left[1\angle Z1L \bullet (I_\phi + k_0 \bullet I_r) \bullet (I_r \bullet e^{j \bullet T})*\right]} \qquad (3)$$

T represents the tilt and is used to address nonhomogeneity of the system. The evaluation of (3) for the fault is shown in Fig. 7.
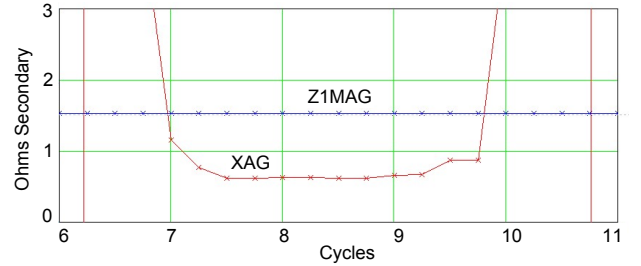
Fig. 7.   Calculated line impedance for Event #1 from Relay W

The line impedance measured by the relay for this fault is 0.62 ohms, or about 40.5 percent of the total line impedance of 1.53 ohms. This correlates to a fault location of 2.76 miles.

We are also interested in the amount of resistance the relay sees during this fault. Equation (4) details the expression used to calculate fault resistance, and Fig. 8 shows the result of the fault resistance calculation.

$$R_F = \frac{\mathrm{Im}\left[V_\phi \bullet (1\angle Z1L \bullet (I_\phi + k_0 \bullet I_r))*\right]}{\mathrm{Im}\left[\frac{3}{2} \bullet (I_{\phi 2} + I_0) \bullet (1\angle Z1L \bullet (I_\phi + k_0 \bullet I_r))*\right]} \qquad (4)$$
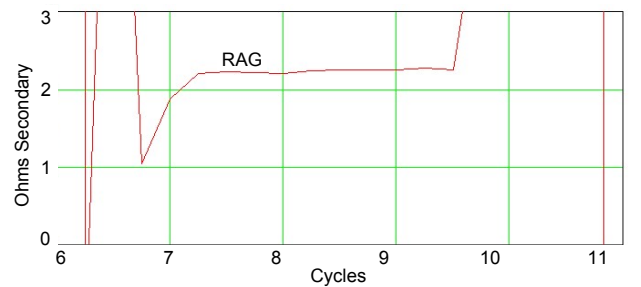
Fig. 8.   Fault resistance for Event #1 as calculated by Relay W

The resistance is shown to be about 2.25 ohms for this fault, which is about 1.5 times the actual impedance of the

line. If we truly had that much fault resistance, how did we have up to 20 percent more fault current than we expected?

3) Relay W Event #1 Phasor Analysis

To get another view of the event, we take a look at the phasor diagram from Relay W at Cycle 8, shown in Fig. 9. The positive-sequence memory voltage (V1MEM) is chosen as the reference. The positive-sequence memory voltage closely resembles A-phase voltage (VA) prior to the fault for a balanced three-phase system.
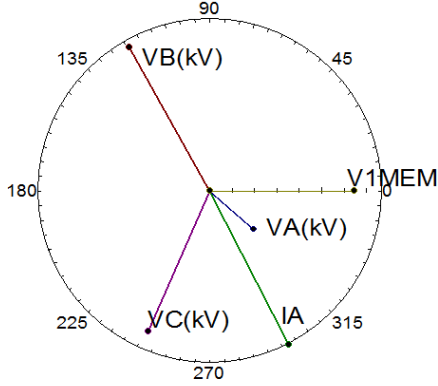
Fig. 9.   Phasor diagram of Event #1 from Relay W

The faulted phase current (IA) lags the faulted phase voltage (VA) by 21.6 degrees. For a bolted A-phase-to-ground fault in front of the relay, we would expect the A-phase current to lag the A-phase voltage by approximately the line angle (Z1ANG). Therefore, if the A-phase current lags the A-phase voltage by much less than Z1ANG, this translates to a large apparent fault resistance.

Additionally, we can see that VA lags V1MEM by about 41.3 degrees. This indicates that the faulted phase voltage shifted from its prefault location. Note that the angular difference between V1MEM and VA affects the impedance calculation of the memory-polarized mho element. The numerator of (2) approaches zero as the angular difference between V1MEM and VA approaches 90 degrees. For most line-to-ground faults, prefault VA and post-fault VA are in phase and only differ in magnitude.

If we change the polarizing quantity and simulate a self-polarized mho element (using VA as the polarizing quantity), the calculated impedance of the mho distance element differs greatly due to the large amount of apparent resistance calculated by the relay. For instance, we can examine the results obtained using different polarizing quantities for a mho element, namely self-polarization and cross-polarization.

The general formula for evaluating the reach of distance elements with various polarizing techniques is given in (5) [3].

$$r = \frac{\text{Re}\left(V \bullet V_p *\right)}{\text{Re}\left[Z \bullet I \bullet V_p *\right]} \tag{5}$$

where:

I = measured current.

V = measured voltage.

V_p = polarizing voltage.

Equation (6) yields the result of a self-polarized mho element. The polarization value becomes the measured faulted phase value.

$$Z\phi G = m \bullet |Z1L| = \frac{\text{Re}\left[V_\phi \bullet \left(V_\phi\right)*\right]}{\text{Re}\left[1\angle Z1L \bullet \left(I_\phi + k_0 \bullet I_r\right) \bullet \left(V_\phi\right)*\right]} \tag{6}$$

The self-polarized mho element calculates an impedance of 2.8 ohms, which exceeds the line impedance of 1.53 ohms. This indicates that a self-polarized mho element would not have overreached. The numerator of a self-polarized mho element is not affected by the phase shift between prefault and post-fault voltages.

Equation (7) shows the calculation for a cross-polarized mho element. The polarization value becomes the phase-to-phase voltage from the unfaulted phases, shifted by 90 degrees.

$$Z\phi\phi G = m \bullet |Z1L| = \frac{\text{Re}\left[V_\phi \bullet \left(V_{\phi j \bullet PP}\right)*\right]}{\text{Re}\left[1\angle Z1L \bullet \left(I_\phi + k_0 \bullet I_r\right) \bullet \left(V_{j \bullet PP}\right)*\right]} \tag{7}$$

The cross-polarized mho element evaluates to 1.17 ohms, which is less than the 1.3-ohm reach of Z1G. This indicates that the cross-polarized element would overreach for this fault as well. In fact, it has a greater overreach than the memory-polarized element. Voltage VBC shifted 90 degrees will be in phase with VA prefault. During the fault, as VA begins to lag the polarizing quantity, the numerator in (7) diminishes, creating the potential for an overreach. Fig. 10 shows the results and comparison of the three polarizing quantities.
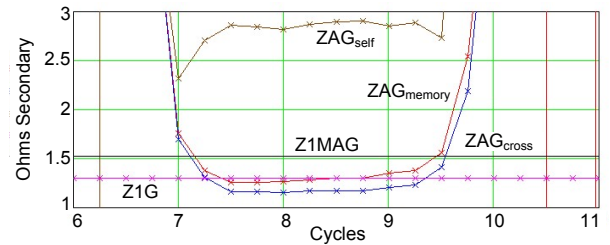
Fig. 10.   Distance elements of Event #1 from Relay W

The shift in voltage contributed to the memory-polarized ground mho element overreach. Why did the A-phase voltage shift? Is the potential transformer (PT) performing poorly? One way to answer these questions is to examine the response of another relay to the same fault.

B. Relay Y Analysis for the Most Recent Fault

Relay Y, a line current differential relay communicating with Relay Z, cleared the fault correctly. Fig. 11 shows the data from Event #1 for Relay Y.
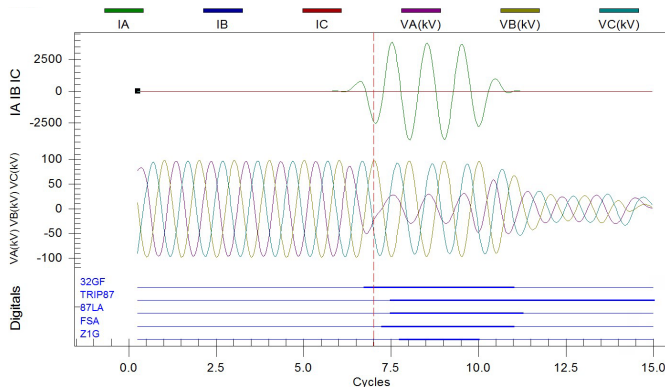
Fig. 11.   Event #1 from Relay Y

We can see that this relay operated immediately on line current differential for A-phase (87LA). The relay saw the fault in the forward direction (32GF), and the Zone 1 backup ground mho also operated (Z1G). There is no load current present prior to the fault because the remote terminal of the line was open.

The phasor diagram from Relay Y at Cycle 8 is shown in Fig. 12.
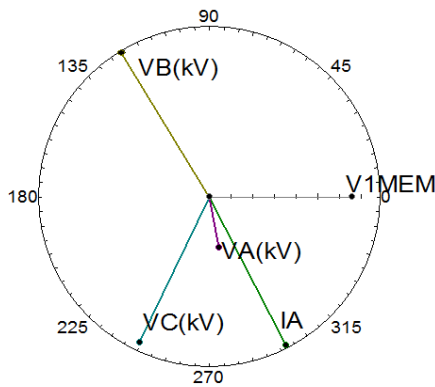
Fig. 12.   Phasor diagram of Event #1 from Relay Y

This relay sees a more pronounced shift in the A-phase voltage than Relay W did, to the point that the faulted phase voltage is lagging the faulted phase current. The relay settings for Relay Y (same for Relay Z) are shown as follows:

CTR = 240
PTR = 1400.00
Z1MAG = 0.76
Z1ANG = 80.26
Z1MG = 0.68
Z0MAG = 2.05
Z0ANG = 72.17
LL = 5.92

The results from similar analysis to that performed on Relay W are shown for Relay Y in Table I.

The relay reported a fault location of –1.98 miles, which corresponds to the negative reactance measured. This indicates the fault was on Line AB, but the line current differential correctly cleared the fault on Line BC. The negative reactance

measured is created by the faulted phase voltage lagging the faulted phase current. This fault appears to have challenged the impedance-based fault location in the relay.

TABLE I
CALCULATION RESULTS FROM EVENT #1 FOR RELAY Y

Z_2	–4.5 ohms (forward)
$\angle I_2 - \angle I_0$	0° (FSA)
Memory-Polarized Reach	0.19 ohms
Resistance	1.35 ohms
Reactance	–0.25 ohms
Self-Polarized Reach	–20 ohms
Cross-Polarized Reach	0.1 ohms
Fault Location	–1.98 miles

The self-polarized mho element does not operate for this fault due to the large negative value for the impedance created by the phase relationship between the faulted phase voltage and faulted phase current. IA current, which in this case is equal to I_r in (6), leads VA voltage by about 15 degrees. We then compensate this IA current by the line angle setting of 80 degrees, which causes the compensated line current to lead the faulted phase voltage by more than 90 degrees, which will lead to a negative calculated impedance.

With two relays at two separate locations reporting a shifted faulted phase voltage, it seems unlikely there is a faulty PT. In addition, we can rule out capacitance voltage transformer (CVT) transients creating an issue for the following two reasons:

- Substation A uses traditional PTs.
- The angular relationships are present throughout the event report, not just within the first 2 cycles.

C. Relay Z Event Prior to Reclose

Up to this point, we have studied Relay W and Relay Y for the overreaching trip. We now turn our attention to Relay Z for the initial trip. Fig. 13 shows the phasor diagram from Relay Z at Cycle 8.
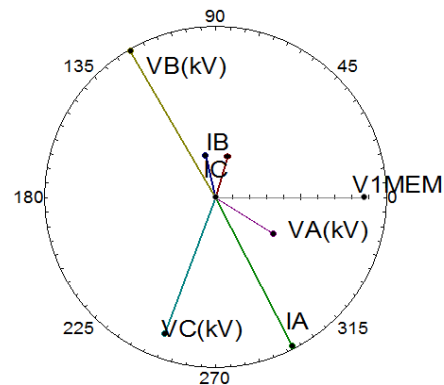
Fig. 13.   Phasor diagram from Relay Z initial trip at Cycle 8

We see that the A-phase voltage is lagging 30 degrees from its prefault state. This verifies this is due to an event on the power system and not the result of instrument transformer error.

D. Tabulated Evaluations for All Eight Faults on Line BC Seen From Relay W, Relay Y, and Relay Z

Table II shows a summary of the quantities evaluated for all eight faults, with the two misoperations highlighted. In Table II, Z_2 is the negative-sequence impedance, R is the apparent resistance, and X is the apparent line impedance.

We can make the following observations from the relays involved in these faults:

- All relays see a forward fault.
- All relays report a fault resistance greater than the line impedance for all faults seen.
- The self-polarized (SP) mho element properly restrains for all faults, but appears to be unreliable for internal faults.
- The cross-polarized (CP) mho element overreaches more than the memory-polarized (MP) distance element.
- Relay Y is closest to the fault and at times sees a negative reactance.
- This was a power system event, and it was not caused by faulty measurement devices.

E. Double-Ended Fault Location Using Negative-Sequence Values

The fault location values reported by the relays are inaccurate. Relay Y reports a fault location behind the relay, while it is apparent from the event reports that the fault was in fact in the forward direction. To try to better determine the actual location of the fault, we use the double-ended negative-sequence impedance method described in [5].

Because Substation B is load only, we use the event reports from Substations A and C to determine the fault location. It is important to note that Substation A has a PT ratio (PTR) of 800/1 while Substations B and C have PTRs of 1400/1 (all current transformer ratios [CTRs] are 240/1). Going forward, we normalize all secondary impedances using a PTR of 800/1. This means we need to convert Line BC impedance by multiplying it by 1400/800, which makes Line BC secondary impedance equal $1.33\angle80.25$ ohms. The total positive-sequence line impedance from Substation A to Substation C is then $2.86\angle80.45$, and the total line length is 12.71 miles. The results are shown in Table III with per-unit fault location (*m*) and fault location in miles from Substation A and Substation B.

The double-ended negative-sequence fault location indicates all faults are on the Line BC section at an average distance of 1.68 miles from Substation B.

The fault location reported by Relay W is consistently less than the fault location reported by the double-ended method by 25 to 30 percent.

TABLE II
COMBINED DATA FROM ALL FAULTS

	Relay W						Relay Y						Relay Z					
Event	Z_2	R	X	SP Reach	CP Reach	MP Reach	Z_2	R	X	SP Reach	CP Reach	MP Reach	Z_2	R	X	SP Reach	CP Reach	MP Reach
1	−6.6	2.25	0.62	2.8	1.17	1.26	−4.5	1.35	−0.25	−20	0.1	0.19						
2	−9.9	3.38	1.35	4	2	2.23							−2.6	1	0.45	1.28	0.68	0.77
3	−6.7	2.5	1.03	3	1.6	1.76												
4	−9.2	3.2	1.4	3.8	2	2.3							−2.7	1	0.45	1.27	0.68	0.77
5	−6.6	2.25	0.6	2.8	1.14	1.25	−4.5	1.38	−0.27	−15	0.08	0.17						
6	−9.8	3.2	1.33	3.8	1.99	2.2	−6.3	1.9	0.23	3.2	0.62	0.8	−2.7	1	0.46	1.29	0.7	0.78
7	−7	2.6	1.2	3.2	1.81	1.99												
8	−9.9	3.45	1.55	4	2.25	2.5							−2.6	0.97	0.38	1.23	0.6	0.69

TABLE III
DOUBLE-ENDED FAULT LOCATION RESULTS

	Calculated Double-Ended Fault Location			Relay Fault Location (miles)	
Event	Miles From A	Miles From B	Miles From C	Relay W	Relay Z
2	8.26	1.46	4.45	5.98	3.48
4	8.39	1.59	4.32	6.28	3.44
6	8.13	1.34	4.58	5.84	3.68
8	9.15	2.36	3.56	6.7	2.9

IV. INTERCIRCUIT FAULT

Because this does not look like a traditional phase-to-ground fault, we are left trying to determine what can cause a high apparent fault resistance and greater than normal expected fault current. After the initial analysis, it was revealed that the 161 kV line had a 69 kV underbuild line that was owned by another utility. The owner of the 69 kV underbuild line was contacted a few months after the fault occurred and asked if they had any event reports that corresponded with the fault on the 161 kV line. As it turned out, the 69 kV line had a digital relay that captured two events that correspond to the 161 kV events. There may have been more, but many newer events had pushed older events out of the relay.

The faults retained in the 69 kV relay correspond to the two most recent events seen by Relay W. First, we look at Event #2, which occurred prior to the reclose, as shown in Fig. 14.
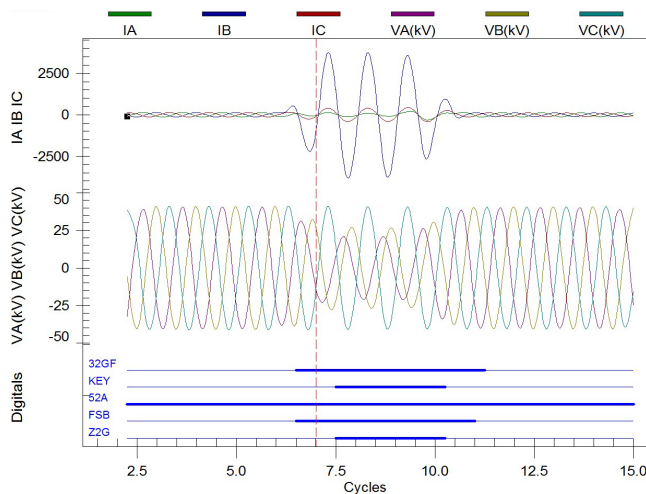
Fig. 14. Event #2 from the 69 kV relay

This event occurred at 12:10:06.399, which is the same time that Event #2 from Relay W occurred. Fortunately, the 69 kV relay was also connected to a Global Positioning System (GPS) clock, as was Relay W. The 69 kV relay sees what appears to be a B-phase-to-ground fault (FSB). However, B-phase and A-phase voltages are depressed, which is unexpected. The relay identifies the fault in the forward direction (32GF) and as being within the reach of Zone 2 (Z2G). Fig. 15 shows the phasor diagram during the fault from the 69 kV relay at Cycle 8.

VA and VB have shifted toward each other, while VC remains unchanged from the prefault value. Also, the faulted B-phase current lags the faulted phase voltage by 150 degrees, which far exceeds the 65-degree lag phase relationship we would expect for a forward B-phase-to-ground fault (Z1ANG = 65). If we combine this event with Event #2 from Relay W, as shown in Fig. 16, we see what appears to be a phase-to-phase fault.
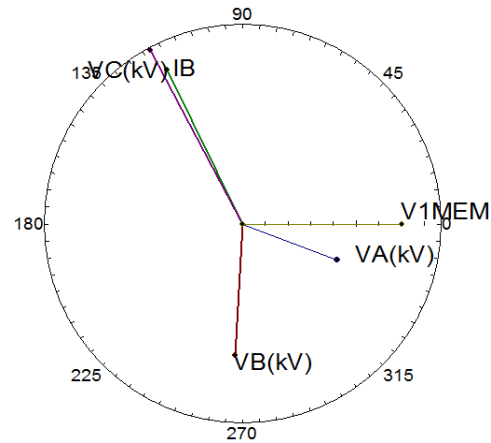
Fig. 15. Phasor diagram of Event #2 from the 69 kV relay
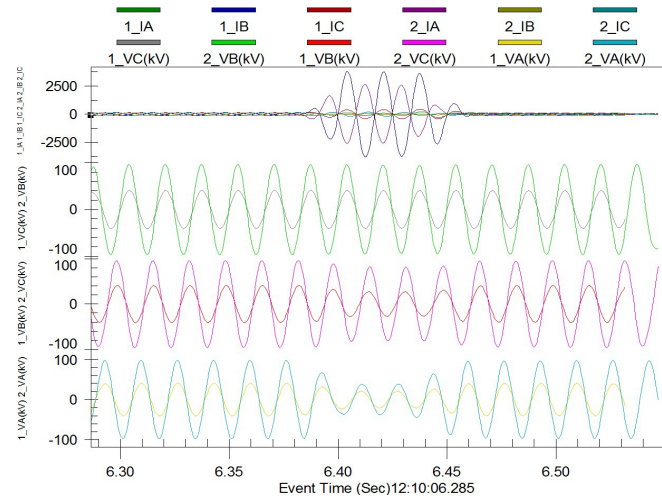
Fig. 16. Combined Event #2 from Relay W and the 69 kV relay, where 1 is the 69 kV relay and 2 is Relay W

The time-synchronized event clearly shows that the 161 kV and 69 kV lines came in contact with each other. A-phase of the 161 kV line is out of phase with B-phase of the 69 kV line.

We are also able to recognize that the phase rotation of the two power systems is different. The 161 kV system has an ACB phase rotation, while the 69 kV system has an ABC phase rotation.

From the perspective of the 161 kV system, this looks like an A-phase-to-C-phase fault, while from the 69 kV system, it looks like an A-phase-to-B-phase fault. For convenience, we swap the C- and B-phases on the 161 kV system going forward and consider this an A-phase-to-B-phase intercircuit fault.

Finally, we review the combined event report for Event #1, shown in Fig. 17.

Again, we can see that the two events coincide with each other. For this event, Breaker 4 is open (see Fig. 1), which appears to have changed the characteristics of the fault.
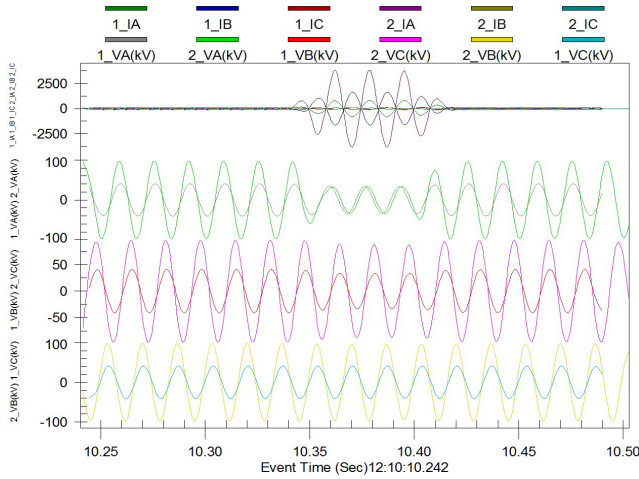
Fig. 17. Combined Event #1 from Relay W and the 69 kV relay, where 1 is the 69 kV relay and 2 is Relay W

An intercircuit fault led to an undesirable operation of Relay W. Fig. 18 shows the fault with both the 161 kV and 69 kV systems. It is important to note that the 69 kV system is simplified for convenience.
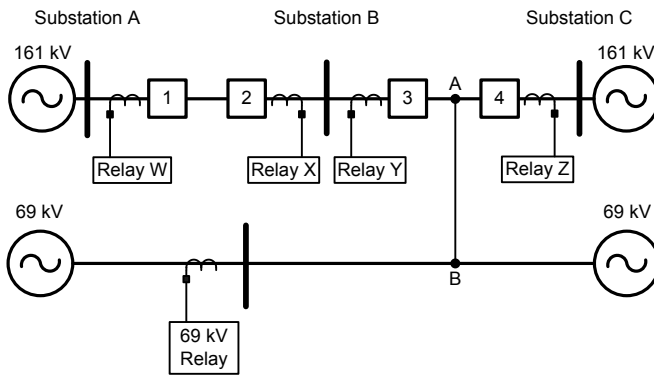
Fig. 18. Intercircuit fault between 161 kV and 69 kV systems

Indeed, the A-phase-to-B-phase fault makes some sense based on the line construction and phase connections. Fig. 19 shows the tower construction for the portion of the line indicated by the double-ended fault location method with the phasing and fault connection marked.
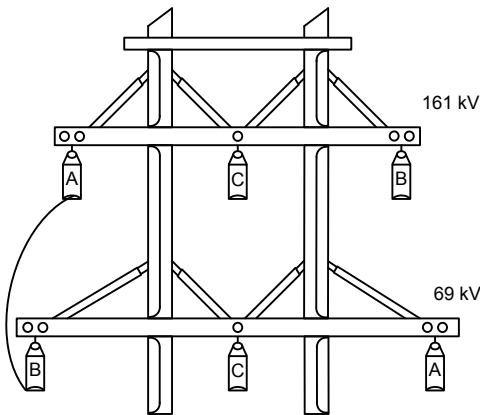
Fig. 19. Tower construction

Without event reports, GPS time, and offline analysis tools, it would have been very difficult, if not impossible, to determine the root cause of this operation. With modern technology, we are able to see more and therefore learn more about the power system.

We want to know more about this type of fault and the voltage and current phasors it can produce.

V. SYMMETRICAL COMPONENT ANALYSIS

To verify the analysis, we use symmetrical components to solve for the currents and voltages seen during an intercircuit fault.

First, we start by defining the equations for symmetrical components, referenced to A-phase with ABC phase rotation [6], where $\alpha = 1e^{j120°}$.

$$\begin{bmatrix} I_0 \\ I_1 \\ I_2 \end{bmatrix} = \frac{1}{3} \begin{bmatrix} 1 & 1 & 1 \\ 1 & \alpha & \alpha^2 \\ 1 & \alpha^2 & \alpha \end{bmatrix} \begin{bmatrix} I_A \\ I_B \\ I_C \end{bmatrix} \tag{8}$$

Also, we define the phase quantities as they are defined by the sequence quantities.

$$\begin{bmatrix} I_A \\ I_B \\ I_C \end{bmatrix} = \begin{bmatrix} 1 & 1 & 1 \\ 1 & \alpha^2 & \alpha \\ 1 & \alpha & \alpha^2 \end{bmatrix} \begin{bmatrix} I_0 \\ I_1 \\ I_2 \end{bmatrix} \tag{9}$$

Another method to express phase quantities in terms of symmetrical components is shown in (10). Notice that the alpha operator is removed and each sequence component is shown in terms of its respective phase.

$$I_A = I_{0a} + I_{1a} + I_{2a}$$
$$I_B = I_{0b} + I_{1b} + I_{2b} \tag{10}$$
$$I_C = I_{0c} + I_{1c} + I_{2c}$$

Fig. 20 shows a vectorial representation of this relationship.
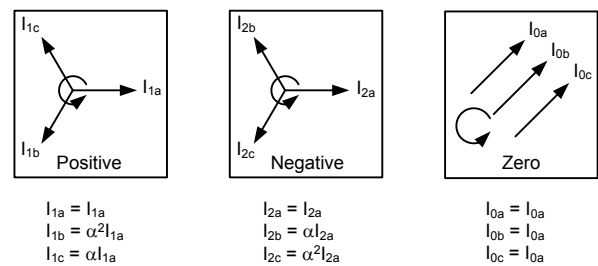
Fig. 20. Phasor relationship for sequence components

When dealing with intercircuit faults, it is easier to remove the alpha operators, solve for sequence components, and then convert back to the reference phase as needed.

For example, when solving for I_{1b} and expressing it in terms of I_{1a}, we multiply I_{1b} by α (or divide by α^2). This shifts I_{1b} to be in phase with I_{1a}. We can define multipliers to move between the different sequence quantities to get the desired reference, which for our purposes is A-phase. Table IV shows the multipliers we use to convert B_{BASE} components and C_{BASE} components to A_{BASE} components. Note that this matches the vectorial relationship in Fig. 20.

TABLE IV
SEQUENCE COMPONENT MULTIPLIERS

Sequence	A-Phase	B-Phase	C-Phase
Positive	1	α	α^2
Negative	1	α^2	α
Zero	1	1	1

Next, we define two three-phase lines. Line 1 has A-phase coming in contact with B'-phase on Line 2, as shown in Fig. 21.
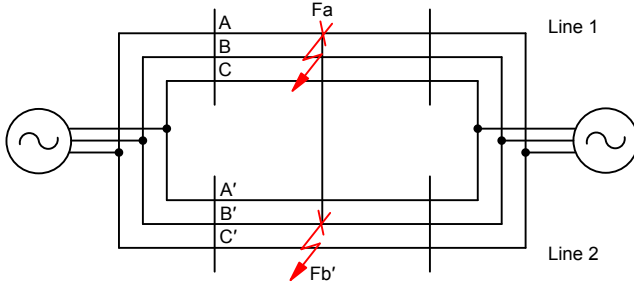
Fig. 21.   Basic three-line diagram

Fig. 22 shows a sequence impedance representation of the system.
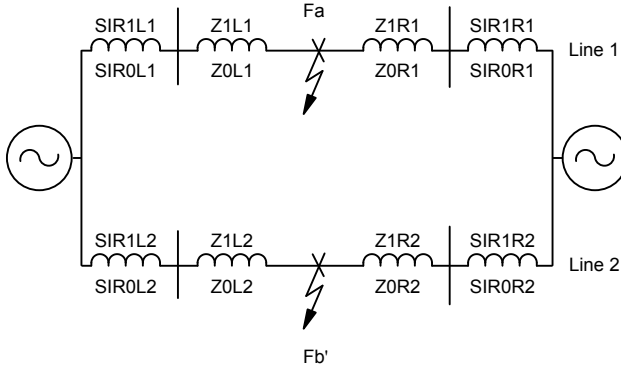
Fig. 22.   One-line diagram of system impedances

At the point of the fault (Fa and Fb'), if the fault resistance is zero, V_A equals $V_{B'}$ and I_A equals $-I_{B'}$. All other phases will have no current because we assume a no-load condition.

Now that we have defined the constraints for this type of fault, we arrive at the following conclusions when looking at the formulas for the sequence networks.

$$\begin{aligned}
\left(I_{0b'} + I_{1b'} + I_{2b'} \right) &= -\left(I_{0a} + I_{1a} + I_{2a} \right) \\
\left(V_{0a} + V_{1a} + V_{2a} \right) &= \left(V_{0b'} + V_{1b'} + V_{2b'} \right)
\end{aligned} \quad (11)$$

Based on these constraints, we connect the A sequence networks in series (a+, a–, a0) and the B' sequence networks in series (b'+, b'–, b'0). Then we parallel the total A network to the total B' network.

Another key point is to select the correct values for the voltage source in the positive-sequence A network and the positive-sequence B' network. The positive-sequence voltage generated in the B' network leads the positive-sequence voltage generated in the A network by 240 degrees (ABC rotation). Therefore, we select the source of the A network to be $1\angle 0$ and the B' network to be $1\angle 240$. With this information, we are able to construct the total sequence network for this fault, as shown in Fig. 23.
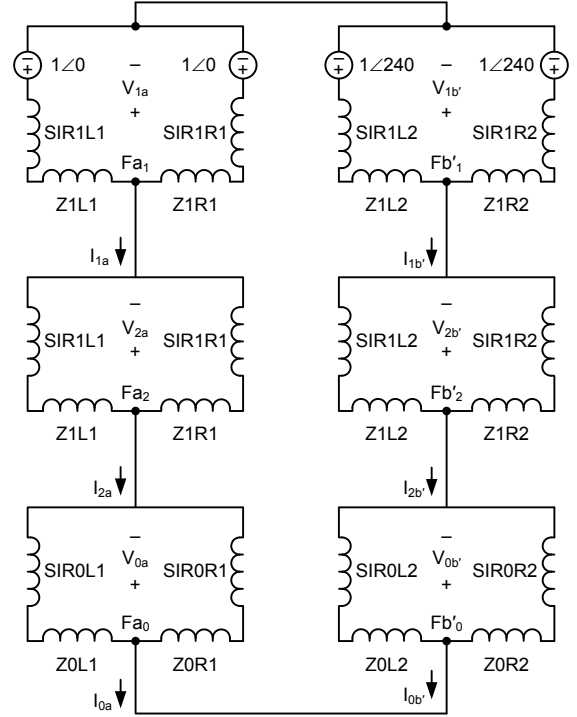
Fig. 23.   Total diagram of sequence impedances for AB' intercircuit fault

We can simplify Fig. 23 into a Thévenin equivalent by performing series parallel connections as shown in Fig. 24. In this diagram, Z_{1a} represents the Thévenin equivalent of the A-phase positive-sequence network at the point of the fault, Fa.
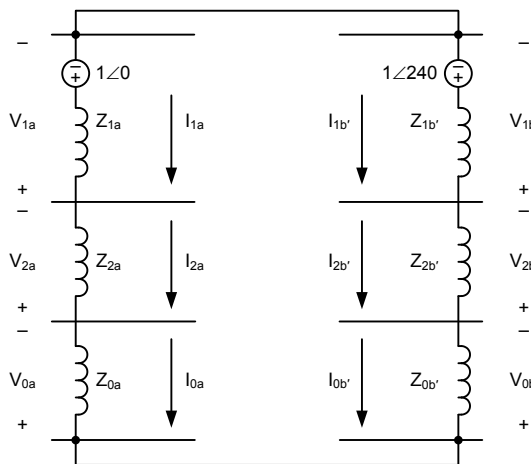
Fig. 24.   Thévenin equivalent AB' intercircuit fault

To solve for I_{1a}, we simply sum the voltage drops around the loop.

$$I_{1a} = \frac{(1\angle 0 - 1\angle 240)}{(Z_{1a} + Z_{2a} + Z_{0a} + Z_{1b} + Z_{2b} + Z_{0b})} \qquad (12)$$

This can be simplified to:

$$I_{1a} = \frac{\sqrt{3}\angle 30}{Z_T} \qquad (13)$$

Z_T is a summation of all the sequence impedances. It can be seen that for a fully reactive system, the current I_{1a} evaluates to an angle of –60 degrees relative to the A-phase positive-sequence voltage. This is due to the subtraction of the two-source voltages involved in creating a 30-degree shift in the numerator of (12). It can also be seen that if A-phase came in contact with A'-phase at the same voltage base, no fault current would flow because the numerator of (12) would evaluate to zero. However, if A-phase and A'-phase are at different voltage levels, circulating current can flow between A-phase and A'-phase.

VI.   Differences Between Intercircuit, Simultaneous, and Cross-Country Faults

At this point, it is important to recognize that an intercircuit fault is a single fault event occurring between two circuits. If either phase comes in contact with ground (AB'G), then we would treat this as two simultaneous ground faults (AG, B'G). For simultaneous faults, the constraints would change at the point of the fault such that $V_A = V_{B'} = 0$ and the faulted phases, I_A and $I_{B'}$, would be calculated simultaneously because they would no longer be equal to each other. Reference [7] details a method to solve for these types of faults.

A cross-country fault is a type of simultaneous fault in which two faults occur at two separate geographical locations.

VII.   Analysis of Intercircuit Faults

We will now perform some basic analysis and review relay element operations for a simple system.

A.   Conversion to A-Phase Reference

For further analysis, it is necessary to convert all sequence quantities to A_{BASE}. This conversion is required to solve for sequence quantities on each line so that they can be compared. Using Fig. 20 as a reference, we perform the following to shift all B_{BASE} components to A_{BASE} components:

$$\begin{aligned} I_{1a'} &= I_{1b'} \cdot \alpha & V_{1a'} &= V_{1b'} \cdot \alpha \\ I_{2a'} &= I_{2b'} \cdot \alpha^2 & V_{2a'} &= V_{2b'} \cdot \alpha^2 \\ I_{0a'} &= I_{0b'} & V_{0a'} &= V_{0b'} \end{aligned} \qquad (14)$$

A similar method can be used to shift C_{BASE} components, also using Fig. 20. A-phase components require no shift.

B.   Example Calculations

Refer to the appendix in this paper for example calculations for the simple system shown in Fig. 25. To simplify the example compared to the real-world event, the same voltage base is used for the A and B' networks going forward. Also, the positive-sequence and zero-sequence source impedances are equal. Rather than showing SIR1L1 and SIR0L1 in Fig. 25, they are equal and referred to as SIRL1.
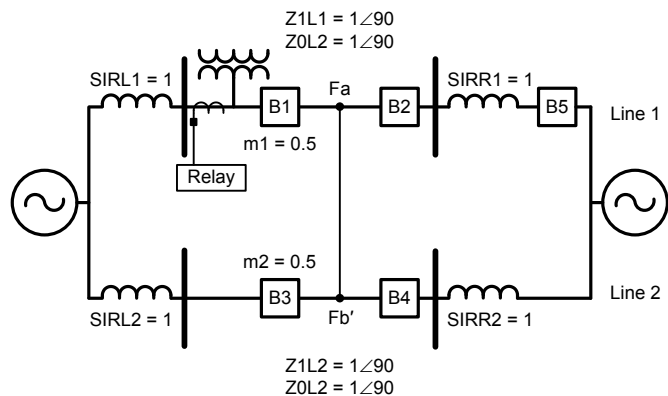
Fig. 25.   Example system

The example system in Fig. 25 is reduced to an equivalent system, as shown in Fig. 26.
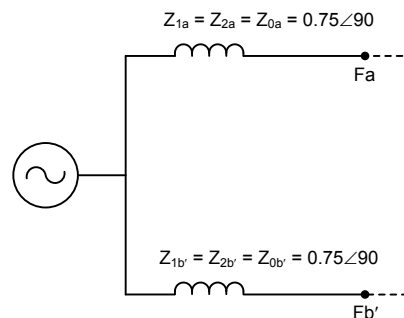
Fig. 26.   Simplified impedance diagram

The fault voltages and fault currents at Points Fa and Fb', as calculated in the appendix, are shown in Fig. 27.
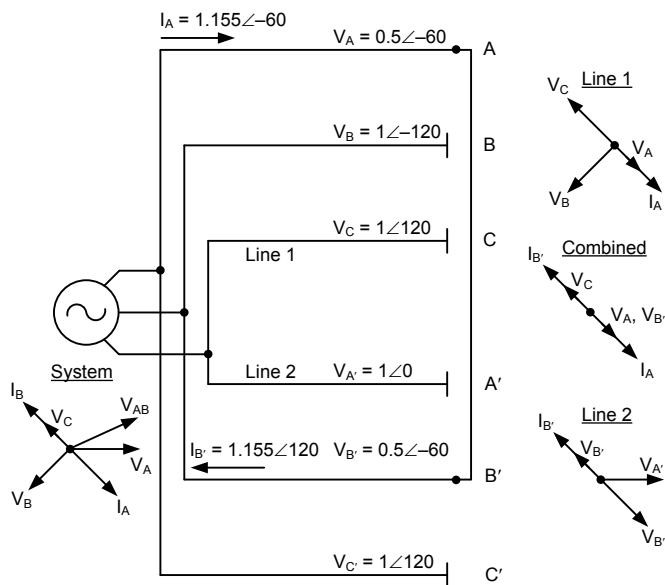
Fig. 27.   Fault voltages and fault currents for total system equivalent

At the point of the fault, if a relay were able to see both faulted phases (the combined phasors), this would clearly look like a phase-to-phase fault. However, the relays on Line 1 and Line 2, which only see the voltage and current on their respective lines, essentially see half of the phase-to-phase fault.

C. Solve for System Equivalent Fault Type

We can now view this fault from the perspective of the system and solve for an equivalent fault type.

If we calculate the system sequence components on A_{BASE} with the given system phase current values from Fig. 27, we get the following sequence components, where I_{1ST} is the positive-sequence system current, I_{2ST} is the negative-sequence system current, and I_{0ST} is the zero-sequence system current:

$$I_{1ST} = 0.667\angle-90$$
$$I_{2ST} = 0.667\angle-30 \tag{15}$$
$$I_{0ST} = 0$$

We can also solve for I_{1ST} (summation of I_{1a} and $I_{1b'}$) and I_{2ST} by using I_{1a} from (12) and the proper multipliers found in (14).

$$I_{1ST} = \left(I_{1a} - \alpha \bullet I_{1b'}\right)$$
$$I_{2ST} = \left(I_{1a} - \alpha^2 \bullet I_{2b'}\right) \tag{16}$$
$$I_{0ST} = \left(I_{1a} - I_{0b'}\right)$$

Factoring out the alpha term and noting $I_{1a} = -I_{1b'} = -I_{2b'} = -I_{0b'}$:

$$I_{1ST} = \left(\sqrt{3}\angle-30 \bullet I_{1a}\right) \tag{17}$$

$$I_{2ST} = \left(\sqrt{3}\angle30 \bullet I_{1a}\right) \tag{18}$$

$$I_{0ST} = 0 \tag{19}$$

Replacing I_{1a} with (13):

$$I_{1ST} = \frac{3}{Z_T} \tag{20}$$

$$I_{2ST} = \frac{3\angle60}{Z_T} \tag{21}$$

$$I_{0ST} = 0 \tag{22}$$

I_A and I_B can then be expressed in terms of I_{1ST} and I_{2ST} as follows:

$$I_A = I_{1ST} + I_{2ST} + I_{0ST} \tag{23}$$

$$I_A = \frac{\left(3\bullet\sqrt{3}\angle30\right)}{Z_T} \tag{24}$$

$$I_B = -I_A \tag{25}$$

$$I_A - I_B = \frac{\left(6\bullet\sqrt{3}\angle30\right)}{Z_T} \tag{26}$$

The apparent impedance to the fault using the line-to-line voltage (infinite source) and line-to-line current is shown in (27).

$$\frac{V_{AB}}{I_{AB}} = Z_1 \tag{27}$$

$$\frac{\sqrt{3}\angle30}{2.31\angle-60} = Z_1 \tag{28}$$

$$Z_1 = 0.75\angle90 \tag{29}$$

Note that when applying (26) and $V_A - V_B = \sqrt{3}\angle 30$ to (27), we find that $V_{AB}/I_{AB} = Z_T/6$. So, a system phase-to-phase element essentially sees the average of all sequence impedances as the apparent Z_1. In our example system, with all impedances being equal, the apparent Z_1 is accurate. This shows that while there is no zero-sequence current from the perspective of the system, the zero-sequence impedance of the lines affects the apparent Z_1 seen by a relay looking at both lines, which is interesting to note. Also, this shows we could solve for the system fault current by using $Z_T/6$ as Z_1 and Z_2 and solving for a system A-phase-to-B-phase fault, placing Z_1 and Z_2 in parallel, as shown in Fig. 28.

$$Z_1 = Z_2 = \frac{Z_T}{6} \tag{30}$$

$$I_{1ST} = \frac{1}{\left(Z_1 + Z_2\right)} \tag{31}$$

$$I_{2ST} = -I_{1ST} \bullet \alpha^2 \tag{32}$$

Note that (20) and (21) yield the same results as (31) and (32).
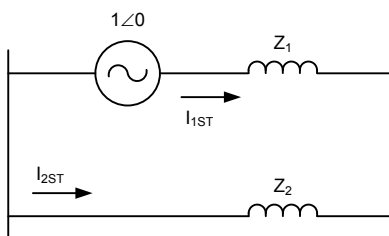
Fig. 28.   Sequence diagram for phase-to-phase fault

Remember that extra care is required to solve intercircuit fault problems with lines that have a common bus. In our example, we are considering the two lines as isolated. However, this is a simplification for the purpose of the example. In practice, there will be a system impedance behind the faulted lines and voltage drops in the system that are a function of A and B' current.

VIII. EVALUATION OF DISTANCE ELEMENTS FOR AB' INTERCIRCUIT FAULT AND A-PHASE-TO-GROUND FAULT FOR EXAMPLE SYSTEM

The voltages and currents at the relay location in Fig. 25 for an AB' intercircuit fault and A-phase-to-ground fault at Point Fa are as follows (see the appendix):

$$
\begin{aligned}
V_{Arelay} &= 0.577\angle -30 \\
V_{Brelay} &= 1\angle -120 \\
V_{Crelay} &= 1\angle 120 \\
I_{Arelay} &= 0.577\angle -60
\end{aligned} \tag{33}
$$

In comparison, the fault values seen by the relay for a bolted A-phase-to-ground fault at Point Fa are as follows:

$$
\begin{aligned}
V_{Arelay} &= 0.333\angle 0 \\
V_{Brelay} &= 1\angle -120 \\
V_{Crelay} &= 1\angle 120 \\
I_{Arelay} &= 0.667\angle -90
\end{aligned} \tag{34}
$$

Notice that they are similar in that the A-phase voltage is depressed and the A-phase current is elevated. However, the phase angle relationship is very different between the two fault types.

With the expected fault values calculated at m1 = 0.5 and m2 = 0.5, we can determine the reach of self- and memory-polarized distance elements for these fault types using (2) and (6). For illustration purposes, we show the mho circle with expansion for the memory-polarized element. The expansion from the origin can be found by using (35), assuming no prefault current [8].

$$SIRexpansion = \frac{-\left(V1_{prefault} - V1_{fault}\right)}{I1_{fault}} \tag{35}$$

For our example, the V1 prefault is $1\angle 0$. The SIRexpansion for the AB' intercircuit fault is shown in (36).

$$\frac{-\left(1\angle 0 - 0.577\angle -30\right)}{0.577\angle -60} = 1\angle -90 \tag{36}$$

The SIRexpansion for the A-phase-to-ground fault is shown in (37).

$$\frac{-\left(1\angle 0 - 0.333\angle 0\right)}{\left(0.667\angle -90\right)} = 1\angle -90 \tag{37}$$

The intercircuit fault and phase-to-ground fault see the same SIRexpansion for the sample system. If the reach of the element is set at 1 pu with a maximum torque angle (MTA) of 90 and SIRexpansion of $1\angle -90$, the center of the circle is at 0,0 with a radius of 1.

A. Self-Polarized Mho Element for Internal Fault

Fig. 29 shows the performance of a self-polarized mho element with the reach set at 100 percent line length for an A-phase-to-ground fault at Point Fa and an AB' intercircuit fault at Fa to Fb'.

As expected, the A-phase-to-ground fault is plotted at 0.5 pu of the line (brown dot), which is exactly where the fault is located. The self-polarized mho element trips the breaker for this fault. The intercircuit fault lies just outside the reach of the element (blue dot). This is problematic because we will **not** trip for this fault using the self-polarized mho element. This shows the lack of dependability we can have with a self-polarized mho element for an intercircuit fault. We can also see that the AB' intercircuit fault does not follow the MTA of the ground element, even though in this case the relay determines that the fault is phase to ground.
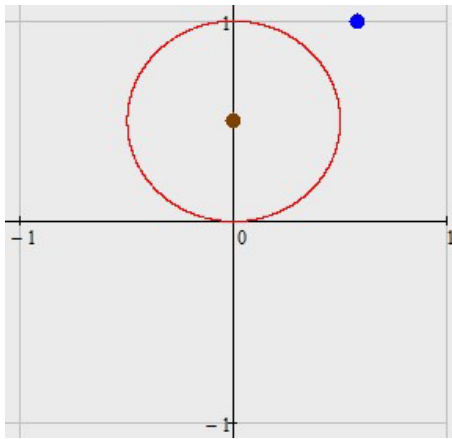
Fig. 29. Self-polarized mho characteristic for A-phase-to-ground fault and AB' intercircuit fault at 50 percent of Line 1

B. Memory-Polarized Element for Internal Fault

Fig. 30 shows the response of the memory-polarized mho element at the moment of greatest expansion for the same fault. For reference, the self-polarized mho characteristic is also plotted.
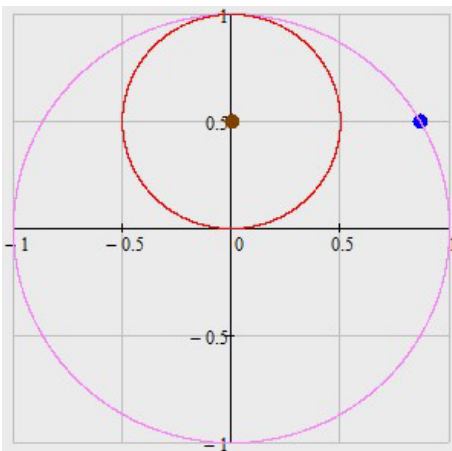
Fig. 30. Memory-polarized mho reach for A-phase-to-ground fault and AB' intercircuit fault at 50 percent of Line 1

Again, as expected, the A-phase-to-ground fault plots at 0.5 pu, the exact location of the fault (brown dot). However, we can see that the memory-polarized expansion is so large in this system that it is on the edge of picking up this mho element for an AB' intercircuit fault. For this particular fault at 50 percent of the line, tripping for an AB' intercircuit fault is desirable for dependability. However, even the memory-polarized element lacks dependability for faults greater than 50 percent of the line length. For faults beyond 50 percent of the line, Zone 2 elements may provide clearing of the fault.

C. Distance Element Performance for External Fault

For the same system, we set the reach at 85 percent and simulate a fault at 115 percent of the line. First, we look at the performance of the memory-polarized elements as shown in Fig. 31.
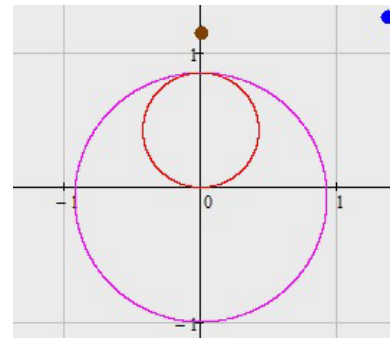
Fig. 31. Memory-polarized mho reach for A-phase-to-ground fault and AB' intercircuit fault at 115 percent of Line 1

For the fault at 115 percent of the line, the memory-polarized element properly restrains, apparently giving us security for the fault beyond the line. However, recall that the utility experienced an issue when the 161 kV line was singled-ended. In Fig. 32, we simulate the AB′ fault with Breaker 5 (shown in Fig. 25) open.
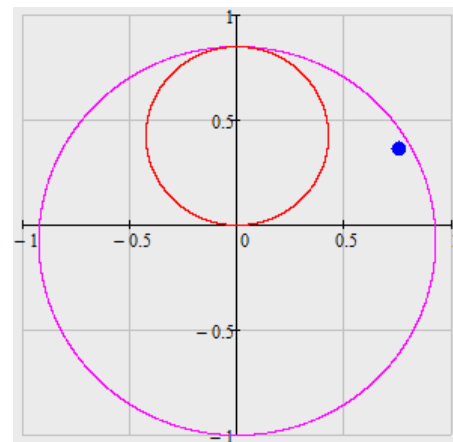
Fig. 32. Memory-polarized mho reach for A-phase-to-ground fault and AB' intercircuit fault at 115 percent of Line 1 with Breaker 5 open

The memory-polarized element overreaches for an AB' intercircuit fault when the line is single-ended, and this leads to a misoperation. In addition, the magnitude of the AB' fault current is 35 percent larger than an A-phase-to-ground fault at the same location. Due to the low trajectory angle of the intercircuit fault apparent impedance in the ground mho element, it is possible to use load-encroachment logic on Zone 1 ground elements to add security for an external intercircuit fault.

The apparent reactance is 0.38 pu ohms, which causes the single-ended fault locator to severely underestimate the location of the fault by 66 percent. The resistance calculated is 0.797 pu ohms.

The simple system provides similar results to the operation of Relay W regarding mho element performance and fault locator performance.

As we can see, there are challenges with mho element dependability for in-zone intercircuit faults as well as challenges with mho element security for out-of-zone intercircuit faults. In addition, the reactance calculations are unreliable for single-ended impedance-based fault location.

IX. SOLUTIONS

The following subsections offer solutions for intercircuit faults.

A. Protection

The easiest and most straightforward way to properly operate during an intercircuit fault is to install line current differential on both lines (161 kV and 69 kV). Line current differential properly restrains for intercircuit faults outside of the zone of protection and reliably trips for faults within the zone of protection. The particular tower construction of this line has portions in which intercircuit faults are possible and should receive additional consideration for a line current differential scheme.

Even if line current differential is used, it is still likely that mho elements will be used for backup protection. Therefore, a detailed study to set distance elements based on the possibility of an intercircuit fault should be considered. To increase security for external intercircuit faults, we could reduce the reach of Zone 1 elements or use load encroachment, but that would adversely affect sensitivity and dependability for traditional fault types. Another way to increase security for external intercircuit faults would be to time-delay Zone 1 by 10 cycles to allow any adjacent line time to clear the fault. However, this would sacrifice speed for traditional faults. To increase dependability for in-zone intercircuit faults, we might need to expand the reach of the Zone 1 element, which would affect security for traditional fault types and possibly for external intercircuit faults. Another option, which would not affect security for traditional fault types, is to accept clearing in-zone intercircuit faults with Zone 2 elements.

It can be seen that it could be very difficult, if not impossible, to have distance relays operate with speed, sensitivity, security, and dependability for traditional fault types and intercircuit fault types. With the difficulties encountered when considering an intercircuit fault type, can they simply be ignored?

There are two questions to ask in this regard:
1. *How likely is it that an intercircuit fault will occur?*
   In general, intercircuit faults are very unlikely, but a small possibility exists for them to occur on lines that share a right of way. Certain horizontal line constructions (as was the case for this fault) are more susceptible to creating an intercircuit fault when conductor sags occur. Sags can be caused by hot days with high load or by ice and snow accumulation on the line. Vertical line construction during high crosswind conditions may be more susceptible to an intercircuit fault. The aforementioned faults are generally temporary in nature, which is a point to consider when contemplating the consequences of the fault. Other, more catastrophic conditions that could increase the likelihood of an intercircuit fault are tornadoes or vehicle (plane) crashes, which are permanent faults. Either way, the protection engineer should endeavor to quantify the possibility of an intercircuit fault.

2. *If an intercircuit fault occurs, what are the consequences?*
   Because the mho element may underreach during an in-zone intercircuit fault, it is possible the fault will be cleared on a time-delayed Zone 2 element (assuming no communications scheme is available when the fault occurs). This exposes the system to the fault longer than expected, which could lead to equipment damage and/or a loss of system stability. Because the mho element may overreach during an external intercircuit fault, overtripping can occur. Overtripping can lead to system stability issues or an undesired loss of load. In this example, Substation B, which had load, was lost due to the overreach of Relay W.

Depending on the likelihood and consequences of an intercircuit fault, different courses of action can be taken. In general, the occurrence rate will be very low, but it is important for the protection engineer to examine the consequences of an intercircuit fault by including this fault type in the study.

If it is determined that the consequences are not severe, it may be reasonable for the protection engineer to accept possible miscoordination for this rare fault type.

However, adverse or severe consequences may warrant a reevaluation of the protection system being deployed. Loss of critical load, loss of system stability, or equipment damage could warrant the use of two line current differential systems with alternate communications paths for the best security and dependability during an intercircuit fault.

B. Fault Location

Due to the low apparent reactance seen during an intercircuit fault, traditional impedance-based fault location will not be accurate. There are two options to remedy this.

1) Double-Ended Negative-Sequence Fault Location

This method is still accurate for intercircuit faults and can be processed offline after the fault. Because the phasors are available in the model previously created for an intercircuit fault, we are able to use (38) to validate this method [9], where V_{2S} and I_{2S} equal negative-sequence voltage and current measured at Breaker 1 in Fig. 25 and V_{2R} and I_{2R} are the negative-sequence voltage and current measured at Breaker 2 in Fig. 25.

$$m = \frac{\overline{V_{2S}} - \overline{V_{2R}} + \overline{I_{2R}} \cdot \overline{Z_{2L}}}{\overline{Z_{2L}} \cdot \left(\overline{I_{2S}} + \overline{I_{2R}} \right)} \tag{38}$$

For all simulated faults with both ends closed in, the formula in (38) gives the exact fault location. In practice, there will be errors in relay measurement, system models, CT and PT accuracy, and so on. In general, results should be within ±10 percent of the actual fault location.

2) Traveling Wave Fault Location

This method tags the arrival time of a wave peak at a local terminal and compares it with the time of arrival at the remote terminal end. To solve for the fault location, we need the

speed of the wave propagation (near the speed of light), the known distance of the line, and an accurate time stamp (within ±500 nanoseconds gives the most accurate results). This method is also immune to fault type because it simply looks at the wave front from the sampled current.

If it had been installed on all line terminals for this fault, a line current differential relay that uses traveling wave fault detection and double-ended negative-sequence fault location would have provided an accurate location of the fault on each line immediately following the fault.

C. GPS Synchronized Time

It is desirable to have GPS clocks at both the 161 kV and 69 kV terminals so intercircuit faults can be more easily identified and analyzed. Sometimes GPS time is required per local regulations, but whenever two circuits share the same right of way, GPS time can be invaluable in analysis and can allow the implementation of traveling wave fault location. In addition, a precise clock provides precise fault location results for traveling wave fault location.

D. Automatic Event Retrieval and Storage

During this major storm, one utility recorded over 300 relay operations in less than one day. Many of the records from earlier in the day were pushed out of the relay memory and lost. If the events had been stored, further analysis could have been pursued. In addition, sometimes analysis does not occur until well after the initial fault, increasing the possibility of losing needed event data. In this event, the owner of the 69 kV line was not contacted until months after the fault occurred. Having an automated event retrieval system, particularly during abnormal weather events, can ensure that all pertinent data are captured and saved.

X. CONCLUSION

Intercircuit faults are rare events, but when they occur, distance element dependability and security can become compromised and impedance-based fault location can be incorrect. Protection engineers must be aware of the consequences of an intercircuit fault to provide the best protection scheme for their application.

The event reports from three relays were analyzed in detail using a math program to better understand the characteristics of the fault from the perspective of the relay, providing the following observations:
- Upon first observation of the waveform, the fault appeared to be an A-phase-to-ground fault.
- The phasor view of the event revealed that the faulted phase voltage had shifted significantly.
- We were able to determine through analysis that the shifted voltage contributed to the following:
  - Ground mho element overreach.
  - High apparent fault resistance.
  - Low apparent line impedance.
  - Incorrect fault location.

- The magnitude of the fault current was higher than expected based on system studies.
- The event analysis led us to ask the following questions:
  - Why did the voltage shift?
  - Why is the fault current higher than expected?

Once it was determined there was underbuild on the line, the utility that owned the underbuild was contacted and an event was found that matched the time stamp of an event on the 161 kV system, which clearly shows the two circuits came in contact with each other.

Symmetrical components were used to validate the voltage and current relationship as seen by the 161 kV relay, validate the use of double-ended negative-sequence fault location, and compare the operation of memory-polarized and self-polarized mho elements.

The following ideal solutions are offered to eliminate misoperations for intercircuit faults:
- Use line current differential.
- Use traveling wave and/or double-ended fault location.

Traditional mho element protection can have conflicting setting guidelines when attempting to provide fast, secure, dependable, and sensitive protection for traditional fault types and intercircuit fault types. Intercircuit faults should not be ignored. The consequences of this type of fault should be known so that proper decisions can be made about the protection scheme.

This paper also discusses additional improvements such as GPS timing and automated event retrieval.

XI. APPENDIX

This appendix provides example calculations for the simple system shown in Fig. 25. Recall that SIRL1 = SIR1L1 = SIR0L1.

Find the Thévenin equivalent at the point of the fault.

$$Z_{1a} = \frac{(1\angle 90 + 0.5\angle 90)\bullet(1\angle 90 + 0.5\angle 90)}{(1\angle 90 + 0.5\angle 90)+(1\angle 90 + 0.5\angle 90)} = 0.75\angle 90$$

For this example, $Z_{1a} = Z_{2a} = Z_{0a} = Z_{1b'} = Z_{2b'} = Z_{0b'}$.
Solve for I_{1a}.

$$I_{1a} = \frac{\sqrt{3}\angle 30}{4.5\angle 90}$$

$$I_{1a} = I_{2a} = I_{0a} = 0.385\angle -60$$

The phase currents at Point Fa are as follows:

$$I_A = I_{1a} + I_{2a} + I_{0a}$$

$$I_A = 1.155\angle -60$$

$$I_B = 0$$

$$I_C = 0$$

The phase currents at Point Fb' are as follows:

$$-I_{1a} = I_{1b'} = I_{2b'} = I_{0b'} = 0.385\angle120$$

$$I_B = I_{1b'} + I_{2b'} + I_{0b'}$$

$$I_{A'} = I_{1b'} \cdot \alpha + I_{2b'} \cdot \alpha^2 + I_{0b'} = 0$$

$$I_{B'} = 1.155\angle120$$

$$I_{C'} = 0$$

The sequence voltages at Point Fa are as follows:

$$V_{1a} = 1 - I_{1a} \cdot Z_{1a} = 0.764\angle-10.9$$

$$V_{2a} = -I_{2a} \cdot Z_{2a} = 0.289\angle-150$$

$$V_{0a} = -I_{0a} \cdot Z_{0a} = 0.289\angle-150$$

The sequence voltages at Point Fb' are as follows:

$$V_{1a'} = \left(1\angle240 - I_{1b'} \cdot Z_{1b'}\right) \cdot \alpha = 0.764\angle10.9$$

$$V_{2a'} = \left(-I_{2b'} \cdot Z_{2b'}\right) \cdot \alpha^2 = 0.289\angle-90$$

$$V_{0a'} = \left(-I_{0b'} \cdot Z_{0b'}\right) \cdot 1 = 0.289\angle30$$

The phase voltage and phase current at Point Fa are as follows:

$$V_A = V_{1a} + V_{2a} + V_{0a} = 0.5\angle-60$$

$$V_B = 1\angle-120$$

$$V_C = 1\angle120$$

$$I_A = 1.155\angle-60$$

Notice at the point of the fault (Fa) that the A-phase voltage and A-phase current are in phase and shifted 60 degrees from the V_{1a} reference of 0 degrees. Because I_B and $I_C = 0$, this fault can be mistaken for a phase-to-ground fault.

The voltages and currents at the relay location for the AB' intercircuit fault are as follows:

$$I_{1a}B1 = \text{positive-sequence current from B1}$$

$$I_{1a}B1 = I_{1a} \cdot \frac{\left(SIR1R1 + Z1R1\right)}{\left(SIR1R1 + Z1R1 + SIR1L1 + Z1L1\right)}$$

$$V_{A\,relay} = 1 - 3 \cdot \left(I_{1a}B1 \cdot SIR1L1\right) = 0.577\angle-30$$

$$V_{B\,relay} = 1\angle-120$$

$$V_{C\,relay} = 1\angle120$$

$$I_{A\,relay} = 3 \cdot I_{1a}B1 = 0.577\angle-60$$

In comparison, the fault values seen by the relay for a bolted A-phase-to-ground fault at Point Fa are as follows:

$$I1gB1 = \text{positive-sequence current for phase-to-ground}$$

fault from B1

$$I1gB1 = \frac{1}{3 \cdot \left(SIR1L1 + Z1L1\right)}$$

$$I1gB1 = 0.222\angle-90$$

$$V_{A\,relay} = 1 - 3 \cdot \left(I1gB1 \cdot SIR1L1\right) = 0.333\angle0$$

$$V_{B\,relay} = 1\angle-120$$

$$V_{C\,relay} = 1\angle120$$

$$I_{A\,relay} = 3 \cdot I1gB1 = 0.667\angle-90$$

XII. REFERENCES

[1] D. Costello and K. Zimmerman, "Determining the Faulted Phase," proceedings of the 63rd Annual Conference for Protective Relay Engineers, College Station, TX, March 2010.

[2] J. Roberts and A. Guzmán, "Directional Element Design and Evaluation," proceedings of the 21st Annual Western Protective Relay Conference, Spokane, WA, October 1994.

[3] E. O. Schweitzer, III and J. Roberts, "Distance Relay Element Design," proceedings of the 46th Annual Conference for Protective Relay Engineers, College Station, TX, April 1993.

[4] J. Mooney and J. Peer, "Application Guidelines for Ground Fault Protection," proceedings of the 24th Annual Western Protective Relay Conference, Spokane, WA, October 1997.

[5] K. Zimmerman and D. Costello, "Impedance-Based Fault Location Experience," proceedings of the 58th Annual Conference for Protective Relay Engineers, College Station, TX, April 2005.

[6] A. Amberg and A. Rangel, "Tutorial on Symmetrical Components, Part 2: Answer Key," May 2014. Available: http://www.selinc.com.

[7] D. Tziouvaras, "Analysis of Complex Power System Faults and Operating Conditions," proceedings of the 35th Annual Western Protective Relay Conference, Spokane, WA, October 2008.

[8] D. Costello, "Lessons Learned Analyzing Transmission Faults," proceedings of the 61st Annual Conference for Protective Relay Engineers, College Station, TX, April 2008.

[9] A. Rangel, "Using an Offline Software Tool for Fault Location Estimation," December 2012. Available: http://www.selinc.com.

XIII. BIOGRAPHY

Ryan McDaniel earned his BS in Computer Engineering from Ohio Northern University in 2002. In 1999, he was hired by American Electric Power (AEP) as a relay technician, where he commissioned protection systems. In 2002, Ryan began working in the Station Projects Engineering group as a protection and control engineer. His responsibilities in this position included protection and control design for substation, distribution, and transmission equipment as well as coordination studies for the AEP system. In 2005, Ryan joined Schweitzer Engineering Laboratories, Inc. and is currently a field application engineer. His responsibilities include providing application support and technical training for protective relay users. Ryan is a registered professional engineer in the state of Illinois and a member of IEEE.